Article

Antimicrobial Properties of the Polyaniline Composites against *Pseudomonas aeruginosa* and *Klebsiella pneumoniae*

Moorthy Maruthapandi [1], Arumugam Saravanan [1], John H. T. Luong [2] and **Aharon Gedanken [1],***

[1] Department of Chemistry, Bar-Ilan Institute for Nanotechnology and Advanced Materials, Bar-Ilan University, Ramat-Gan 52900, Israel; lewismartin.jesus@gmail.com (M.M.); saran.bc94@gmail.com (A.S.)

[2] School of Chemistry, University College Cork, Cork T12 YN60, Ireland; luongprof@gmail.com

* Correspondence: gedanken@mail.biu.ac.il; Tel.: +97-235-318-315; Fax: +97-237-384-053

check for
updates

Abstract: CuO, TiO$_2$, or SiO$_2$ was decorated on polyaniline (PANI) by a sonochemical method, and their antimicrobial properties were investigated for two common Gram-negative pathogens: *Pseudomonas aeruginosa* (PA) and *Klebsiella pneumoniae* (KP). Without PANI, CuO, TiO$_2$, or SiO$_2$ with a concentration of 220 μg/mL exhibited no antimicrobial activities. In contrast, PANI-CuO and PANI-TiO$_2$ (1 mg/mL, each) completely suppressed the PA growth after 6 h of exposure, compared to 12 h for the PANI-SiO$_2$ at the same concentration. The damage caused by PANI-SiO$_2$ to KP was less effective, compared to that of PANI-TiO$_2$ with the eradication time of 12 h versus 6 h, respectively. This bacterium was not affected by PANI-CuO. All the composites bind tightly to the negative groups of bacteria cell walls to compromise their regular activities, leading to the damage of the cell wall envelope and eventual cell lysis.

1. Introduction

Many pathogens often live for considerable periods on inert surfaces to trigger the transmission of infectious diseases, especially in nursing homes, hospitals, and clinical settings, known as nosocomial or healthcare-acquired infections. The combined use of disinfectants and bactericidal surface coatings could drastically decrease the prevalence of bacterial infections. The surfaces of medical devices or objects in common clinical/hospital areas can be coated with antimicrobial materials because they are used or touched almost daily by health care workers. The prevention of microbial contamination is also critical in the food and pharmaceutical industries, a growing global concern. PA, the most common Gram-negative pathogen, causes hospital-related pneumonia in the United States [1]. This facultative anaerobe is well adapted to proliferate in the absence of oxygen using nitrate or nitrite as a terminal electron acceptor [2–4]. Carbapenem-resistant PA is a critical (priority 1) pathogen that infects immunocompromised patients [5] and is linked to ventilator-associated pneumonia and sepsis syndromes. Its adaptable genome also allows PA to attain resistance to different antibiotics [6] and infects the airway, urinary tract, burns, and wounds of immunodeficient patients [7]. KP is the commonest cause of hospital-acquired pneumonia in the United States [8] and pneumonia for inpatient populations. In general, Gram-negative bacteria are more difficult to kill and develop resistance more quickly to antibiotics, compared to Gram-positive counterparts.

Copper occurs as solid metal Cu (0); Cu (I) cuprous ion; Cu (II) cupric ion; and, rarely, Cu (III) [9], and its antimicrobial property was dated back in ancient times [10]. Cu and its alloys serve as

antimicrobial agents for both medical and non-medical purposes [11]. In the presence of air, copper is oxidized to CuO, which can be light-activated at ~720 nm [12] to form radicals that impair the bacterial cell wall. TiO_2 powder or its thin film is stable and photosensitive [13]. TiO_2 surfaces can become antimicrobial materials due to their abundance and non-toxicity. Illuminations of TiO_2 induce the release of several reactive oxygen species, and one of the species is hydroxyl radicals ($\cdot$OH), which is reactive and causing oxidative damage to cellular components, leading to eventual cell lysis. With a bandgap of 3.2 eV [14], the antimicrobial activity of TiO_2 is attained under UV radiation at <385 nm.

Polyaniline (PANI) has received significant interest in diversified applications because of its low cost, biocompatibility, stability, and low toxicity [15–17]. However, PANI materials have some disadvantages, including weak processability and poor mechanical stability [18,19]. Several attempts have been advocated to prepare PANI composite materials with improved activity, physical, and structural properties [20–23]. Metal oxides can bind the polymer chain in the PANI backbone to strengthen polymer stability [23–25] for various pertinent uses [18,25–28].

As a part of our on-going activities, this paper extends the applicability of the PANI composite with CuO, TiO_2, or SiO_2, respectively, against two-Gram negative pathogens: *P. aeruginosa* and *K. pneumoniae*. All Gram-negative bacteria have thin peptidoglycan, which is covered by multiple thin layers of membrane. They are harder to eradicate and quickly develop resistance to antibiotics, compared to Gram-positive bacteria. The polymer composites are characterized by FTIR, XRD, SEM, and zeta potential measurement. A postulated mechanism of the bacterial death is then corroborated and supported by relatable experimental data.

2. Experimental Section

2.1. Materials

All chemicals of analytical grade were purchased from Sigma–Aldrich Israel and used without any other purification.

Synthesis of CDs (Carbon Dots)

CDs were synthesized as described previously [26]. Polyethylene glycol-400 (40 mL) was placed in a glass beaker, which was immersed in an oil bath at 60–70 °C. Sonication was performed by dipping an ultrasonic transducer tip in the liquid. After 2 h of sonication at a 35% amplitude, a yellow color CD solution was attained.

Preparation of PANI: The PANI is often synthesized by a chemical or electrochemical oxidative method in an acidic medium with ammonium/potassium persulfates as initiators [29–33]. Simple and green synthesis of conducting polymers is carried out with CDs as an initiator [34–37]. Resulting stable polymers can also be decorated with various metal oxides by facile ultra-sonication to form polymer-metal oxide composites [38–41]. In brief, aniline (1.0 g) dissolved in 25 mL of 4M HNO_3 was admixed with 3 mL of CDs (5 mg). After illumination with UV light for 48 h, the resulting solution became a blackish-brown slurry. The blackish-brown solid was recovered by filtration, followed by extensive washings with distilled water and dried at room temperature.

Synthesis of PANI-CuO: As-prepared PANI (100 mg in 90 mL of ethanol) was admixed with copper (II) acetate (20.1 mg in 10 mL of deionized water, 0.012 M). The reaction mixture was sonicated until the temperature reached 70 °C. The solution pH of 8.0–9.0 was maintained by adding an ammonia solution as required. When the blue-tinted solution turned blackish brown, it was placed on an ice bath and subject to sonication for 30 min [27,28]. PANI exhibited a zeta potential of +42 mV, as measured by a Malvern Zetasizer Nano-ZS (Malvern Panalytical, Malvern, UK).

PANI-TiO$_2$: An identical reaction was performed using 0.1 g of Ti (IV) isopropoxide, instead of 20.1 mg of copper (II) acetate.

PANI-SiO$_2$: In this synthesis, 0.1 g of tetraethyl orthosilicate was used instead of 20.1 mg of copper (II) acetate.

2.2. Antibacterial Tests

Overnight incubation of *P. aeruginosa* PAO1 and *K. pneumoniae* ATCC 700, 603 were carried out at 37 °C in Luria-Bertani (LB) broth. Detailed information on these two bacterial strains was described in Supporting Information. The antibacterial tests were conducted using a mixture of the polymer composite (500 μL) and the bacterial suspension (500 μL). The mixture was incubated at 37 °C with shaking at 200 rpm (AOSI-2 orbital shaker incubator). An aliquot (100 mL) taken at 0, 3, 6, and 12 h was diluted 10-fold in 20% LB medium and plated on the LB agar plates. The plates were dried and incubated for 16 h at 37 °C. Based on the counting of bacterial colonies at appropriate dilutions, the sum of viable bacteria was calculated by the CFU method. The experiments were performed in triplicate.

2.3. Analytical Techniques

A Transon 27 spectrometer (Bruker, Bremen, Germany) was used to acquire all FTIR spectra of the polymer composites. The crystalline nature of the polymer materials was analyzed using the X-ray diffraction technique by a Bruker AXS D8 Advance diffractometer. All morphologies of the polymer composites were performed using an FEI Magellan 400 L microscope (FEI, Hillsboro, OR, USA). For SEM analysis, a small quantity of the dried powder was placed on a carbon tape, which was attached to a copper strip. The material was coated with gold to improve the conductivity required for SEM imaging.

3. Result and Discussion

In 4M HNO_3, the condition used to synthesize PANI aniline with a pKa of 4.6 should be protonated entirely to form the anilinium ions. The synthesized PANI consists of protonated $-NH_3^+$ and aromatic $-C_6H_5$ groups. Homogeneous nucleation of PANI was initiated by the rapid mixing of the acidic solution containing C-dots form PANI irregular tubes, ca. 400–500 nm [33]. Carbon dots (CDs) with negative charges displayed electrostatic interactions with the anilinium ions [34]. The zeta potential of PANI is +42 mV as indicated earlier (Figure S1).

3.1. Characterization of composites

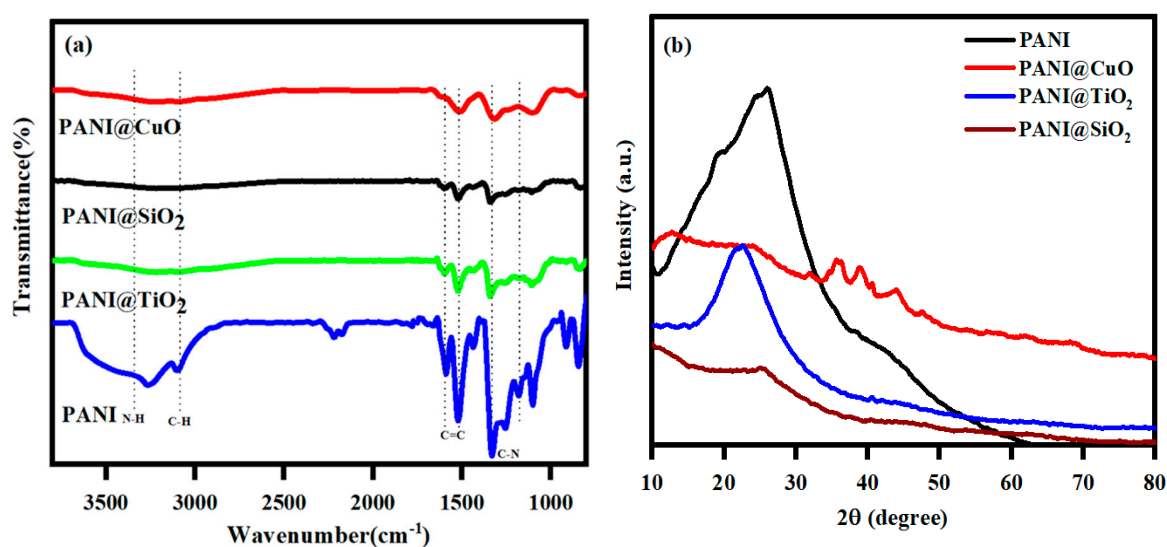FTIR spectra of the polymer composites with major peaks were shown in Figure 1a [35–37] and Table 1.

Figure 1. (**a**) FTIR spectra of the polymer composites and (**b**) XRD pattern for the PANI composites of PANI-CuO, PANI-TiO2, and PANI-SiO2.

Table 1. FTIR peaks and peak assignments of polyaniline (PANI) and its composites.

Materials	Major Peaks and Assignments
PANI	The broad peak at 3272 cm^{-1}, N–H stretching.
	The peak at 3098 cm^{-1}, C–H aromatic stretching vibration.
	The peaks at 1595 and 1516 cm^{-1}, C=C stretching of quinoid and benzenoid rings, respectively.
	The peak at 1331 cm^{-1}, C–N stretching of the secondary aromatic amines.
	The peaks at 1176 and 1252 cm^{-1}, =C–H in-plane vibrations.
	The peak at 825 cm^{-1}, out-of-plane bending of C–H in the 1,4-disubstituted benzene ring.
	The broadband ~1059–1724 cm^{-1}
TiO$_2$ nanoparticles	The broadest one at 3500 cm^{-1}, stretching vibration of the hydroxyl group.
	The second band ~1630 cm^{-1}, bending mode of water Ti–OH.
	The prominent peak at 1383 cm^{-1}, Ti–O modes [42,43].
PANI-TiO$_2$ and PANI-SiO$_2$	The amine stretching vibrations of N–H and C–N stretching are extremely reduced sharp narrow peaks. The aromatic stretching vibration ~3098 cm^{-1} and 1252–1085 cm^{-1} (=C–H in-plane vibration) entirely disappeared due to the strong formation of metal oxides onto the polymer [38].

These reduced intensities and disappearances of the peaks confirmed the development of the polymer composites of CuO, TiO$_2$, and SiO$_2$, with PANI. A vast XRD diffraction peak with 2θ = 20–40° of PANI could be attributed to the periodicity in the polyaniline structure parallel to the polymer chains (Figure 1b). A broad peak of 2θ = 24° was observed for the PANI-SiO$_2$ composite, confirming the formation of SiO$_2$ on the PANI surface (Figure 1a). This polymer composite also showed a significantly reduced intensity compared to the PANI, indicating the formation of a stable composite between SiO$_2$ and the PANI chain. Similar results were also noted for the PANI-TiO$_2$ composite with the lowest intensity. Apparently, the PANI and its related PANI-TiO$_2$ and PANI-SiO$_2$ composite materials were amorphous. The XRD patterns of CuO, TiO$_2$, and SiO$_2$ were reported elsewhere [38–41]. The PANI-CuO also exhibited a reduced diffraction intensity around 2θ = 24°, and the peaks around 2θ = 38–40° are attributed to the CuO.

3.2. Morphology and Particle Size Distribution

As shown in Figure 2, the three PANI composites exhibited irregular morphology with an average diameter of 5 μm. Their corresponding EDX spectra and SEM-EDX elemental analysis spectra confirmed the presence of C, N, O, Au, and Ir, with uniform distribution. For SEM imaging and analysis, the polymer composite material was placed on a carbon tape, which was attached to a copper strip. The anchored composites were then coated with Ir to improve the conductivity required for imaging. Figure 2a,b confirmed the presence of spherical TiO$_2$ particles and small flake-shaped SiO$_2$ particles with the PANI. The SEM-EDS elemental mapping spectra of the three PANI composites further confirmed the presence of Ti and Si (Figure S2).

The presence of C, N, O, and metal ions of Cu, Ti, and Si was observed from the composite XPS spectra as shown in Figure 3. Three new peaks at 838, 123.79, and 886 eV emerged after the adsorption process.
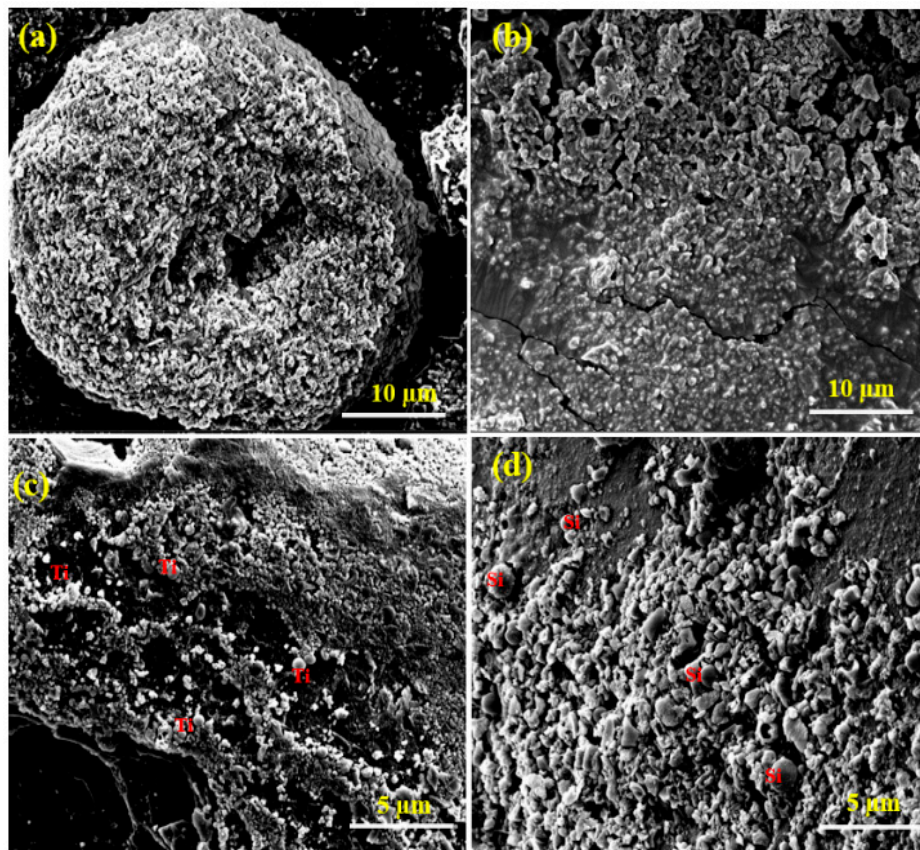
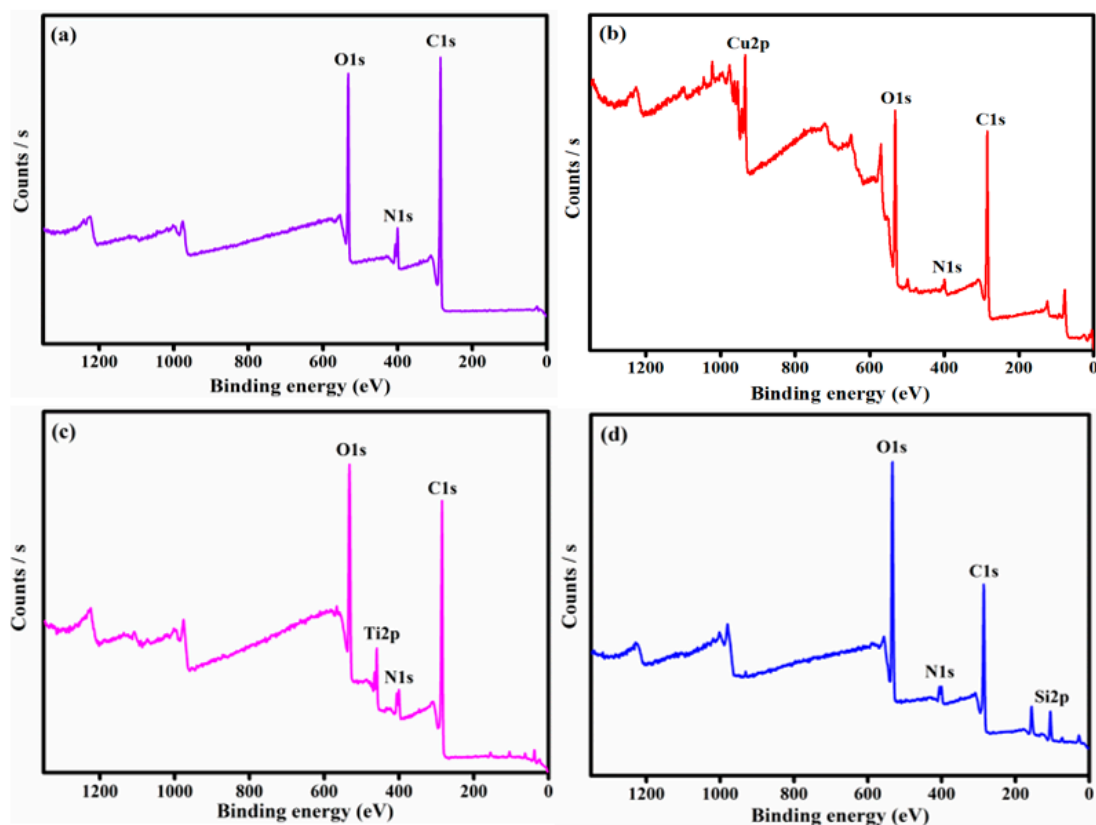**Figure 2.** SEM micrographs of PANI (**a**), PANI-CuO (**b**), PANI-TiO$_2$ (**c**), and PANI-SiO$_2$ (**d**).

Figure 3. The XPS- spectrum of PANI (**a**), PANI-CuO (**b**), PANI-TiO$_2$ (**c**), and PANI-SiO$_2$ (**d**).

3.3. Eradication of P. aeruginosa and K. pneumoniae

There are many literature reports on polymer composites used for eradicating lethal bacteria with metals and metal oxide nanoparticles, such as PANI/polyvinyl alcohol/Ag, PANI@ZnO, PANI/Pt-Pd, PANI/Ag–Pt, PANI-Ag-Au, and Au-PANI -based material [44–48]. However, the synthesis of such polymer- composites is complicated and involves costly noble (Au and Pt) or toxic metals (Ag, and Pd). To avoid the complicated methods and economical cost for the synthesis of PANI composite, the sonochemical method was applied for the formation of highly effective PANI-CuO, PANI-TiO$_2$, and PANI-SiO$_2$. The composites were tested against two Gram-negative bacteria as mentioned earlier. For comparison, the effect of PANI (780 µg/mL), CuO, TiO$_2$, or SiO$_2$ (220 µg/mL, each) was also investigated as the control experiments.

Both PANI-CuO and PANI-TiO$_2$ completely suppressed the growth of PA after 6 h of its exposure to these two composites. The PANI-SiO$_2$ required up to 12 h to eradicate the growth of this bacterium, whereas PANI exhibited a modest antimicrobial effect on PA (Figure 4a). All pure three oxide particles exhibited no antimicrobial activities against PA (Figure 4b). Surprisingly, PANI-CuO showed no antimicrobial activity against KP, whereas PANI-TiO$_2$ completely suppressed the growth of KP after 6 h of exposure (Figure 4c). The growth of KP was not affected by PANI-SiO$_2$ or PANI during the first 6 h incubation but succumbed after 12 h of exposure (Figure 4d).
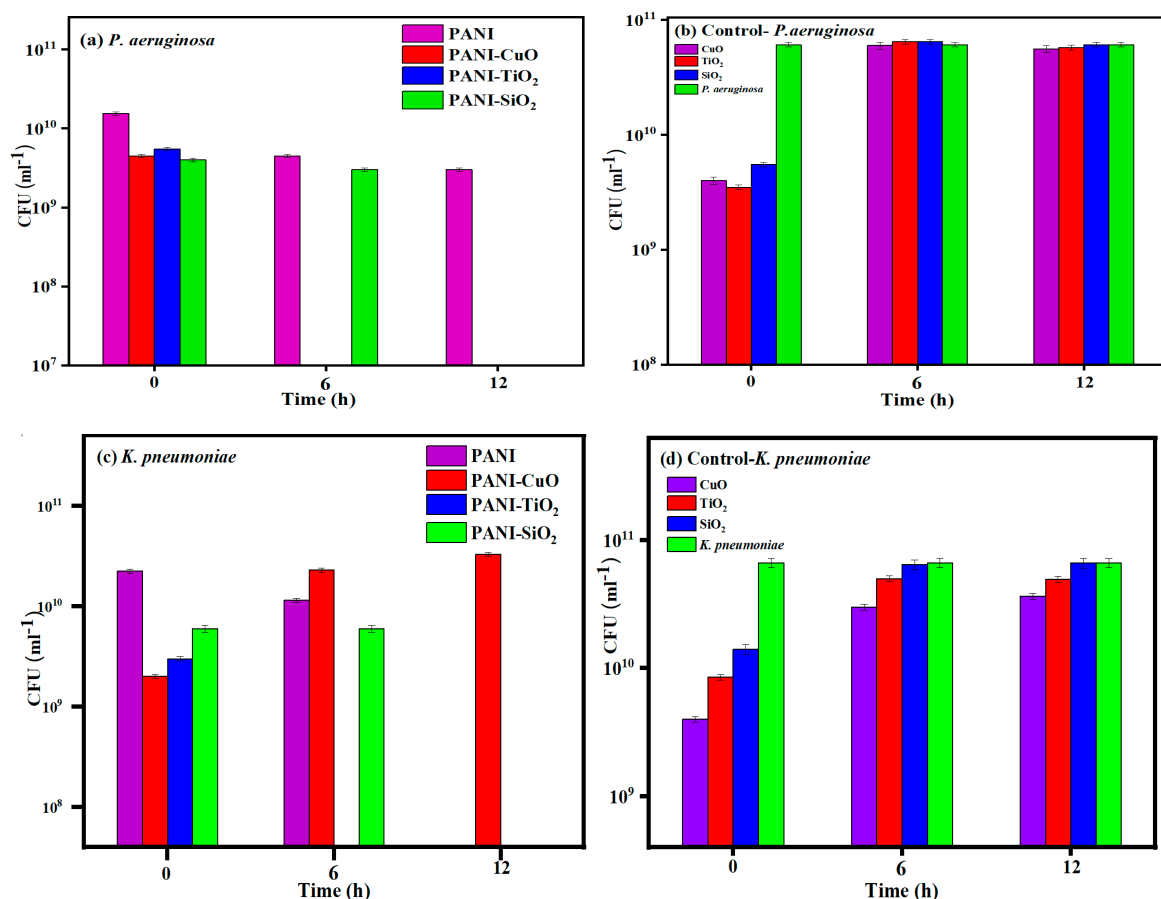

Figure 4. The effect of PANI-CuO, PANI-TiO$_2$, and PANI-SiO$_2$ on the growth of *Pseudomonas aeruginosa* (PA) (**a**) and *Klebsiella pneumoniae* (KP) (**c**). The effect of CuO, TiO$_2$, and SiO$_2$ on PA (**b**) and KP (**d**).

PANI serves as an antimicrobial agent as it exhibits a positive change at pH below 7, which binds to the positively charged membrane of Gram-negative bacteria, consisting of the lipopolysaccharides (LPS). The zeta potential of PA is −29.8 ± 1.5 mV and increases to −25.7 ± 1.4 mV [49] upon its interaction with hexadecyltrimethylammonium bromide (CTAB), a cationic surfactant. Both electrostatic and

hydrophobic interactions between CTAB and the bacterial membrane of PA play an important role that leads to cell lysis [49]. In this context, $-NH_3^+$ and $-C_6H_5$ moieties of PANI bind to the bacterial membrane by electrostatic and hydrophobic interactions, respectively. The hydrophobic domain of PANI, $-C_6H_5$, effectively induces membrane disruption or permeabilization due to its interaction with the membrane hydrophobic core [50]. The binding event compromises the bacterial activities due to the leakage of cellular components, and the breakdown of membrane potential, leading to eventual cell lysis. As a cited example, PANI up to 0.5% (w/v) or 5 mg/mL is needed to subdue the growth and replication of *S. aureus* and *E. coli* and [51]. PANI induces the release of hydrogen peroxide, promoting the liberation of hydroxyl radicals to oxidize bacterial biomolecules, leading to cell lysis. *E. coli* [52] is equipped with a defensive enzyme, catalase, which scavenges hydrogen peroxide to benign water and oxygen. Thus, high PANI concentrations are necessary to promote the H_2O_2 level beyond the scavenging threshold of this enzyme. The PANI concentration used in this study was 0.78 mg/mL, which was significantly below 5 mg/mL, the level needed to eradicate some bacteria as mentioned previously. Nevertheless, this polymer was effective against the growth of KP after 12 h of its exposure but exhibited a very modest effect on the growth of PA.

Without the polymer, both PA and KP were not affected by CuO, TiO_2, and SiO_2 at 220 μg/mL. Several bacteria, including PA and KP, are only suppressed by nano-SiO_2 at concentrations above 0.625 μg/mL [53].

The multidrug-resistant PA [19] can express efflux pumps, β-lactamases, and impermeable outer membrane proteins to overcome the effect of copper ions. The effective Cu concentration against bacteria also depends upon bacterial growth medium compositions and time of exposure. As an example, the minimum inhibitory concentration for $CuSO_4$ copper sulfate for several strains of *E. coli* ranges between 16 and 20 mM (1017–1271 μg/mL) [54]. Both TiO_2 and CuO could bind to the negatively charged bacterial membrane at pH 5 used in the microbial tests. The overall negative charge of two Gram-negative cell walls is attributed to the presence of considerable carboxylic external groups located in bacterial walls. The zeta potential of TiO_2 nanoparticles is 31 ± 0.5 mV at pH 3.0 and approaches 0 at pH = 5.8 ± 0.1 [55]. The surface of the CuO nanoparticles is positively charged between pH 2 and 6 (44.2 ± 1.1 and 36.2 ± 0.9 mV), and approaches neutral at elevated pH 10 [56].

The decoration of CuO, TiO_2, and SiO_2 on PANI should also have some additional effects on the two Gram-negative bacteria, as their cell walls encompass lipids and polysaccharides with low rigidity and strength. The lipopolysaccharides with negative charges are attracted to such oxides with opposite charges. This electrostatic interaction impairs the syntheses of the cell wall, nucleic acids, and proteins, which are required for bacterial growth and replication. The cell membrane is eventually ruptured to release cytoplasmic contents, leading to cell lysis. There was a synergistic effect between PANI and the three oxides, towards the eradication of the two tested Gram-negative bacteria. However, it is not clear whether there is any appreciable amount of reactive oxygen species generated from the polymer composites under ambient light. The bandgap (energy gap) of CuO and TiO_2 is 1.7 and 3.2 eV, respectively, compared to 9 eV for SiO_2 [57]. Thus, CuO can be activated by light with a wavelength of < approx. 720 nm, compared to UV for TiO_2. All the pristine oxides—TiO_2, CuO, and SiO_2—exhibited no antimicrobial activities against PA and KP, as the experiments were simply conducted without light illumination, implying no significant ROS were released under this experimental condition. PANI generates $\pi-\pi^*$ transition under visible light irradiation to transport the exciting electrons into the TiO_2 conduction. The electrons can be moved to an adsorbed electron acceptor to yield oxygenous radicals [58]. The mechanism for the formation of metal oxides by sonochemistry was reported by our group [59,60].

This study focuses on two Gram-negative bacteria, but the synthesized polymer composites can be extended to Gram-positive bacteria. Gram-negative bacteria with a two-membrane barrier are more resistant to antibodies and antibiotics than Gram-positive counterparts [61]. The antimicrobial mechanism of antibiotics generally falls within one of four mechanisms: (i) inhibition or regulation of enzymes involved in cell wall synthesis, (ii) interfering nucleic acid metabolism and repair, (iii) inhibition

of protein synthesis, and (iv) disruption of membrane structure [62]. Emerged multidrug-resistant Gram-negative pathogens pose a significant challenge in the development of new antibiotics and antimicrobial agents. The generation of ROS by metal nanoparticles could be one vital route to overcome the limitation of membrane penetration to kill bacteria. These radicals cause the damage of lipids and proteins and oxidize the deoxynucleotide pool. As mentioned earlier, antibiotics with specific mechanisms of action have been advocated; however, this classical view should be expanded to include the role of ROS generated by metal nanoparticles and polymer composites for bacterial eradication.

A brief discussion was noted here for the toxicity of copper, TiO_2, and SiO_2. Indeed, copper is an essential element for all living organisms, as an adult body contains about 1.2–1.4 mg of copper/kg of body mass. A human can uptake one mg of copper daily, and extra amounts of copper are released in bile and discharged in feces [63]. There is no significant cytotoxicity/inhibition when Chinese hamster lung fibroblast V79 cells are exposed up to 400 ppm of P25 (5.9 nm, 99% anatase), MTI5 (34.1 nm, 80% anatase, and 20% rutile) and bulk TiO_2. TiO_2 nanoparticles (NPs) are aggregated under UV illumination at 254 nm or 365 nm with diminishing photocatalytic activities and exhibit no significant effect on cytotoxicity [64]. The TiO_2 level used in this work was only 220 µg/mL or 220 ppm, below the plausible toxicity level of TiO_2, 400 ppm. The inhibition concentration (IC_{50}) of SiO_2 against U373MG cells U373MG (human glioblastoma cell line) at 24 h has been reported [65]. This value is dependent on the size and surface charges, ranging from 680–6380 µg/mL. Again, such cytotoxic levels are significantly higher than 220 µg/mL used in this work. Based on its non-toxicity, TiO_2 has been formulated in a plethora of industrial and consumer products, including sunscreen lotion, toothpaste, and soap. The U.S. Food and Drug Administration (FDA) has confirmed the safety aspect of TiO_2 in cosmetics, including products intended for use around the eye [66]. Nevertheless, cytotoxicity of any material is concentration-dependent, and its effect is different for different cell lines. Besides various conventional techniques for probing cytotoxicity of materials/nanomaterials, cell-based impedance spectroscopy with multiplexing can be used to probing the cytotoxicity effect of antimicrobial agents for various cell lines. The impedance can be monitored continuously to reflect cell attachment and spreading on a confined electrode surface. The impedance will change drastically when adhered cells are exposed to toxic chemicals and nanomaterials, which impair their attachment and other cell behavior [67–69]. This simple and precise technique provides quantitative data related to cytotoxicity/cytosis for in vitro cell systems in the presence of plausible toxic compounds.

4. Conclusions

CuO, TiO_2, or SiO_2 has no antimicrobial effect against PA and KP. Each PANI composite, however, shows a different antimicrobial activity towards these two Gram-negative bacteria. Both electrostatic and hydrophobic interactions of the PANI composites with the bacterial membrane compromise cell activities, adversely affecting their growth and proliferation. This mechanism is similar to the effect of surfactants on several microorganisms [49,70–72]. PANI also induces the formation of hydrogen peroxide, leading to the production of hydroxyl radicals to oxidize bacterial biomolecules. The release of the above ROS damages bacterial active enzymes, DNA, and proteins that sustain cell proliferation and other important activities [73,74]. The superoxide radical with a negative charge is repulsed by the bacterial membrane with the same charge; therefore, it only acts on the outer surface of bacteria. In contrast, neutral hydrogen peroxide should be able to penetrate the bacterial cell wall to trigger cell lysis.

The use of the polymer composites to prevent the growth of PA is an important finding considering its biofilm formation [75,76], which exhibits intrinsic resistance to different types of chemotherapeutic agents and antibiotics. PA is one of the prime causes of morbidity and mortality in ~80% of patients with cystic fibrosis [77,78]. It is also a common cause of pneumonia infections in intensive care units [79]. PA can form multicellular aggregates or biofilms, which act as a direct barrier to phagocytic cells and antibiotics [80,81]. The application of polymer composites can be extended to a variety of other applications such as food packaging, textile, coating, military, and household equipment.

In practice, the polymer composites can be used in combination to eradicate a mixture of several bacteria. It is paramount important to access the antimicrobial properties against some common multi-drug-resistant bacteria, including foodborne pathogens. Besides *Pseudomonas,* two emerging pathogenic Gram-negative *Enterobacteriaceae* and *Acinetobacter* species are resistant to most available antibiotics [82]. The assessment of the synthesized PANI composites against such pathogens is an important aspect of future endeavors. Of course, other biopolymers and electropolymerized polymers including polypyrrolepropylic acid [83] and poly(*N*-acetyltyramine) [84] could be used to form polymer composites with metal nanoparticles towards the development of a new class of antimicrobial agents.

References

1.   Gordon, A.E.K.; Mathers, A.J.; Cheong, E.Y.L.; Gottlieb, T.; Kotay, S.; Walker, A.S.; Peto, T.E.A.; Crook, D.W.; Stoesser, N. The hospital water environment as a reservoir for carbapenem-resistant organisms causing hospital-acquired infections: A systematic review of the literature. *Clin. Infect. Dis.* **2017**, *64*, 1435–1444. [CrossRef] [PubMed]

2.   Alvarez-Ortega1, C.; Harwood, C.S. Responses of *Pseudomonas aeruginosa* to low oxygen indicate that growth in the cystic fibrosis lung is by aerobic respiration. *Mol. Microbiol.* **2007**, *65*, 153–165. [CrossRef] [PubMed]

3.   Rabaey, K.; Verstraete, W. Microbial fuel cells: Novel biotechnology for energy generation. *Trends Biotechnol.* **2005**, *23*, 291–298. [CrossRef] [PubMed]

4.   Rojo, F. Carbon catabolite repression in *Pseudomonas*: Optimizing metabolic versatility and interactions with the environment. *FEMS Microbiol. Rev.* **2010**, *34*, 658–684. [CrossRef]

5.   Boucher, H.W.; Talbot, G.H.; Bradley, J.S.; Edwards, J.E.; Gilbert, D.; Rice, L.B.; Scheld, M.; Spellberg, B.; Bartlett, J. Bad bugs, no drugs: No ESKAPE! An update from the infectious diseases society of America. *Clin. Infect. Dis.* **2009**, *48*, 1–2. [CrossRef]

6.   Livermore, D.M. Multiple mechanisms of antimicrobial resistance in *Pseudomonas aeruginosa*: Our worst nightmare? *Clin. Infect. Dis.* **2002**, *34*, 634–640. [CrossRef]

7.   Curran, C.S.; Bolig, T.; Torabi-Parizi, P. Mechanisms and targeted therapies for *Pseudomonas aeruginosa* lung infection. *Am. J. Respir. Crit. Care Med.* **2018**, *197*, 708–727. [CrossRef]

8.   Aghamohammad, S.; Badmasti, F.; Solgi, H.; Aminzadeh, Z.; Khodabandelo, Z.; Shahcheraghi, F. First report of extended-spectrum beta-lactamase-producing *Klebsiella pneumoniae* among fecal carriage in Iran: High diversity of clonal relatedness and virulence factor profiles. *Microb. Drug Resist.* **2020**, *26*, 261–269. [CrossRef]

9.   Kiaune, L.; Singhasemanon, N. Pesticidal copper (I) oxide: Environmental fate and aquatic toxicity. *Rev. Environ. Contam. Toxicol.* **2011**, *213*, 21–26.

10.   Borkow, G.; Gabbay, J. Copper, an ancient remedy returning to fight microbial, fungal and viral infections. *Curr. Chem. Biol.* **2009**, *3*, 272–278.

11.   Jung, W.K.; Koo, H.C.; Kim, K.W.; Shin, S.; Kim, S.H.; Park, Y.H. Antibacterial activity and mechanism of action of the silver ion in *Staphylococcus aureus* and *Escherichia coli*. *Appl. Environ. Microbiol.* **2008**, *74*, 2171–2178. [CrossRef] [PubMed]

12.   Baghriche, O.; Rtimi, S.; Pulgarin, C.; Sanjines, R.; Kiwi, J. Innovative TiO$_2$/Cu nanosurfaces inactivating bacteria in the minute range under low-intensity actinic light. *ACS Appl. Mater. Interfaces* **2012**, *4*, 5234–5240. [CrossRef]

13.   Armelao, L.; Barreca, D.; Bottaro, G.; Gasparotto, A.; Maccato, C.; Maragno, C.; Tondello, E.; Štangar, U.L.; Bergant, M.; Mahne, D. Photocatalytic and antibacterial activity of TiO$_2$ and Au/TiO$_2$ nanosystems. *Nanotechnology* **2007**, *18*, 375709. [CrossRef]

14. Puzenat, E. Photo Catalytic Self-Cleaning Materials: Principles and Impact on Atmosphere, EPJ Web of Conferences. *EDP Sci.* **2009**, *1*, 69–74.

15. Monk, P.M.S.; Rosseinsky, D.R.; Mortimer, R.J. Electrochromic Materials and Devices Based on Viologens. In *Electrochromic Materials Devices*; Wiley-VCH Verlag GmbH & Co. KGaA: Weinheim, Germany, 2015; pp. 57–90.

16. Sen, T.; Mishra, S.; Shimpi, N.G. Synthesis and sensing applications of polyaniline nanocomposites: A review. *RSC Adv.* **2016**, *6*, 42196–42222. [CrossRef]

17. Fratoddi, I.; Venditti, I.; Cametti, C.; Russo, M.V. Chemiresistive polyaniline-based gas sensors: A mini review. *Sens. Actuators B Chem.* **2015**, *220*, 534–548. [CrossRef]

18. Qazi, T.H.; Rai, R.; Boccaccini, A.R. Tissue engineering of electrically responsive tissues using polyaniline based polymers: A review. *Biomaterials* **2014**, *35*, 9068–9086. [CrossRef]

19. Ates, M. Review study of electrochemical impedance spectroscopy and equivalent electrical circuits of conducting polymers on carbon surfaces. *Prog. Org. Coat.* **2011**, *71*, 1–10. [CrossRef]

20. Sevilla, F. Chemical sensors based on conducting polymers. In Proceedings of the 2003 Asian Conference on SENSORS-AsiaSENSE 2003, Kebangsann, Malaysia, 18 July 2003; IEEE: Piscataway, NJ, USA; pp. 87–92.

21. Guimard, N.K.; Gomez, N.; Schmidt, C.E. Conducting polymers in biomedical engineering. *Pro. Poly. Sci.* **2007**, *32*, 876–921. [CrossRef]

22. Spitalsky, Z.; Tasis, D.; Papagelis, K.; Galiotis, C. Carbon nanotube-polymer composites: Chemistry, processing, mechanical and electrical properties. *Prog. Polym. Sci.* **2010**, *35*, 357–401. [CrossRef]

23. Kang, H.; Geckeler, K. Enhanced electrical conductivity of polypyrrole prepared by chemical oxidative polymerization: Effect of the preparation technique and polymer additive. *Polymer* **2000**, *41*, 6931–6934. [CrossRef]

24. Hou, Y.; Cheng, Y.; Hobson, T.; Liu, J. Design and synthesis of hierarchical MnO_2 nanospheres/carbon nanotubes/conducting polymer ternary composite for high performance electrochemical electrodes. *Nano Lett.* **2010**, *10*, 2727–2733. [CrossRef] [PubMed]

25. Park, K.-S.; Schougaard, S.B.; Goodenough, J.B. Conducting-polymer/iron-redox- couple composite cathodes for lithium secondary batteries. *Adv. Mater.* **2017**, *19*, 848–851. [CrossRef]

26. Maruthapandi, M.; Saravanan, A.; Luong, J.H.T.; Gedanken, A. Antimicrobial properties of polyaniline and polypyrrole decorated with zinc-doped copper oxide microparticles. *Polymers* **2020**, *12*, 1286. [CrossRef] [PubMed]

27. Ramanavičius, A.; Ramanavičiene, A.; Malinauskas, A. Electrochemical sensors based on conducting polymer-polypyrrole. *Electrochim. Acta* **2006**, *51*, 6025–6037. [CrossRef]

28. Peng, H.; Zhang, L.; Soeller, C.; Travas-Sejdic, J. Conducting polymers for electrochemical DNA sensing. *Biomaterials* **2009**, *30*, 2132–2148. [CrossRef]

29. Mansour, A.F.; Elfalaky, A.; Maged, F.A. Synthesis, characterization and optical properties of PANI/PVA blends. *J. Appl. Phys.* **2015**, *7*, 37–45.

30. Lin, W.; Xu, K.; Xin, M.; Peng, J.; Xing, Y.; Chen, M. Hierarchical porous polyaniline–silsesquioxane conjugated hybrids with enhanced electrochemical capacitance. *RSC Adv.* **2014**, *4*, 39508–39518. [CrossRef]

31. Patil, P.T.; Anwane, R.S.; Kondawar, S.B. Development of electrospun polyaniline/ZnO composite nanofibers for LPG sensing. *Procedia Mater. Sci.* **2015**, *10*, 195–204. [CrossRef]

32. Kawashima, H.; Goto, H. Preparation and properties of polyaniline in the presence of trehalose. *Soft Nanosci. Lett.* **2011**, *1*, 71–75. [CrossRef]

33. Ahmad, S.; Sultan, A.; Raza, W.; Muneer, M.; Mohammad, F. Boron nitride based polyaniline nanocomposite: Preparation, property, and application. *J. Appl. Polym. Sci.* **2016**, *133*, 43989. [CrossRef]

34. Moorthy, M.; Kumar, V.B.; Porat, Z.; Gedanken, A. Novel polymerization of aniline and pyrrole by carbon dots. *New J. Chem.* **2018**, *42*, 535–540. [CrossRef]

35. Maruthapandi, M.; Kumar, V.B.; Gedanken, A. Carbon dot initiated synthesis of poly(4,4′-diaminodiphenylmethane) and its methylene blue adsorption. *ACS Omega* **2018**, *3*, 7061–7068. [CrossRef] [PubMed]

36. Maruthapandi, M.; Kumar, V.B.; Levine, M.; Gedanken, A. Fabrication of poly (4, 4′-oxybisbenzenamine) and its conjugated copolymers initiated by easily accessible carbon dots. *Eur. Polym. J.* **2018**, *109*, 153–161. [CrossRef]

37. Maruthapandi, M.; Luong, J.H.T.; Gedanken, A. Kinetic, isotherm and mechanism studies of organic dye adsorption on poly (4, 4′-oxybisbenzenamine) and copolymer of poly (4,4′-oxybisbenzenamine-pyrrole) macro-nanoparticles synthesized by multifunctional carbon dots. *New J. Chem.* **2019**, *43*, 1926–1935. [CrossRef]

38. Maruthapandi, M.; Nagvenkar, A.P.; Perelshtein, I.; Gedanken, A. Carbon-dot initiated synthesis of polypyrrole and polypyrrole@CuO micro/nanoparticles with enhanced antibacterial activity. *ACS Appl. Polym. Mater.* **2019**, *1*, 1181–1186. [CrossRef]

39. Maruthapandi, M.; Natan, M.; Jacobi, G.; Banin, E.; Luong, J.H.T.; Gedanken, A. Antibacterial activity against methicillin-resistant *staphylococcus aureus* of colloidal polydopamine prepared by carbon dot stimulated polymerization of dopamine. *Nanomaterials* **2019**, *9*, 1731. [CrossRef]

40. Maruthapandi, M.; Sharma, K.; Luong, J.H.T.; Gedanken, A. Antibacterial activities of microwave-assisted synthesized polypyrrole/chitosan and poly (pyrrole-N-(1-naphthyl) ethylenediamine) stimulated by C-dots. *Carbohydr. Polym.* **2020**, *243*, 116474. [CrossRef]

41. Maruthapandi, M.; Eswaran, L.; Luong, J.H.T.; Gedanken, A. Sonochemical preparation of polyaniline@ TiO_2 and polyaniline@ SiO_2 for the removal of anionic and cationic dyes. *Ultrason. Sonochem.* **2020**, *62*, 104864. [CrossRef]

42. Nadica, D.; Abazovic, M.; Comor, M.; Dramicanin, D.; Jovanovic, S.; Jovan, M. Photoluminescence of anatase and rutile TiO_2 particles. *J. Phys. Chem. B* **2006**, *110*, 25366–25370.

43. Mugundan, S.; Rajamannan, G.; Viruthagiri, N.; Shanmugam, R.; Gobi, P. Synthesis and characterization of undoped and cobalt-doped TiO_2 nanoparticles via sol-gel technique. *Appl. Nanosci.* **2015**, *5*, 449–456. [CrossRef]

44. Ghaffari-Moghaddam, M.; Eslahi, H. Synthesis, characterization and antibacterial properties of a novel nanocomposite based on polyaniline/polyvinyl alcohol/Ag. *Arab. J. Chem.* **2014**, *7*, 846–855. [CrossRef]

45. Pandiselvi, K.; Thambidurai, S. Synthesis, Characterization, and antimicrobial activity of chitosan–zinc oxide/polyaniline composites. *Mater. Sci. Semicond. Process.* **2015**, *31*, 573–581. [CrossRef]

46. Boomi, P.; Prabu, H.G.; Mathiyarasu, J. Synthesis, characterization and antibacterial activity of polyaniline/Pt–Pd nanocomposite. *Eur. J. Med. Chem.* **2014**, *72*, 18–25. [CrossRef]

47. Boomi, P.; Prabu, H.G.; Mathiyarasu, J. Synthesis and characterization of polyaniline/Ag–Pt nanocomposite for improved antibacterial activity. *Coll. Surf. B* **2013**, *103*, 9–14. [CrossRef] [PubMed]

48. Boomi, P.; Prabu, H.G.; Manisankar, P.; Ravikumar, S. Study on antibacterial activity of chemically synthesized PANI-Ag-Au Nanocomposite. *Appl. Surf. Sci.* **2014**, *300*, 66–72. [CrossRef]

49. Buzid, A.; Reen, F.J.; Langsi, V.K.; Muimhneacháin, E.O.; O'Gara, F.; McGlacken, G.P.; Luong, J.H.T.; Glennon, J.D. Direct and rapid electrochemical detection of *Pseudomonas aeruginosa* quorum signaling molecules in bacterial cultures and cystic fibrosis sputum samples through cationic surfactant-assisted membrane disruption. *ChemElectroChem* **2017**, *4*, 533–541. [CrossRef]

50. Klibanov, A.M. Permanently microbicidal materials coatings. *J. Mater. Chem.* **2007**, *17*, 2479–2482. [CrossRef]

51. Robertson, J.; Gizdavic-Nikolaidis, M.R.; Swift, S. Investigation of polyaniline and a functionalized derivative as antimicrobial additives to create contamination resistant surfaces. *Materials* **2018**, *11*, 436. [CrossRef]

52. Imlay, J.A. The molecular mechanisms and physiological consequences of oxidative stress: Lessons from a model bacterium. *Nat. Rev. Microbiol.* **2013**, *11*, 443–454. [CrossRef]

53. Kadhum, S.A. The effect of two types of nano-particles (ZnO & SiO_2) on different types of bacterial growth. *Biomed. Pharmacol. J.* **2017**, *10*, 1701–1708.

54. Aarestrup, F.M.; Hasman, H. Susceptibility of different bacterial species isolated from food animals to copper sulphate, zinc chloride and antimicrobial substances used for disinfection. *Vet. Microbiol.* **2004**, *100*, 83–89. [CrossRef] [PubMed]

55. Ramirez, L.; Gentile, S.R.; Zimmermann, S.; Stoll, S. Behavior of TiO_2 and CeO_2 nanoparticles and polystyrene nanoplastics in bottled mineral, drinking and Lake Geneva waters. Impact of water hardness and natural organic matter on nanoparticle surface properties and aggregation. *Water* **2019**, *11*, 721. [CrossRef]

56. Sousa, V.S.; Teixeira, M.R. Aggregation kinetics and surface charge of CuO nanoparticles: The influence of pH, ionic strength and humic acids. *Environ. Chem.* **2013**, *10*, 313–322. [CrossRef]

57. Vella, E.; Messina, F.; Cannas, M.; Boscaino, R. Unraveling exciton dynamics in amorphous silicon dioxide: Interpretation of the optical features from 8 to 11 eV. *Phys. Rev. B* **2011**, *83*, 174201. [CrossRef]

58. Zhang, H.; Zong, R.; Zhao, J.; Zhu, Y. Dramatic visible photocatalytic degradation performances due to synergetic effect of TiO₂ with PANI. *Environ. Sci. Technol.* **2008**, *42*, 3803–3807. [CrossRef] [PubMed]

59. Applerot, G.; Lellouche, J.; Lipovsky, A.; Nitzan, Y.; Lubart, R.; Gedanken, A.; Banin, E. Understanding the antibacterial mechanism of CuO nanoparticles: Revealing the route of induced oxidative stress. *Small* **2012**, *8*, 3326–3337. [CrossRef]

60. Perelshtein, I.; Applerot, G.; Perkas, N.; Wehrschuetz-Sigl, E.; Hasmann, A.; Gübitz, G.; Gedanken, A. CuO–cotton nanocomposite: Formation, morphology, and antibacterial activity. *Surf. Coat. Technol.* **2009**, *204*, 54–57. [CrossRef]

61. Zgurskaya, H.I.; Löpez, C.A.; Gnanakaran, S. Permeability barrier of Gram-negative cell envelopes and approaches to bypass it. *ACS Infect. Dis.* **2015**, *1*, 512–522. [CrossRef]

62. Reygaert, W.C. An overview of the antimicrobial resistance mechanisms of bacteria. *AIMS Microbiol.* **2018**, *4*, 482–501. [CrossRef]

63. Borkow, G.; Gabbay, J. Putting copper into action: Copper-impregnated products with potent biocidal activities. *FASEB J.* **2004**, *18*, 1728–1730. [CrossRef] [PubMed]

64. Male, K.B.; Hamzeh, M.; Montes, J.; Leung, S.C.W.; Luong, J.H.T. Monitoring of potential cytotoxic and inhibitory effects of titanium dioxide using on-line and non-invasive cell-based impedance spectroscopy. *Anal. Chim. Acta* **2013**, *777*, 78–85. [CrossRef] [PubMed]

65. Kim, J.-E.; Kim, H.; An, S.S.A.; Maeng, E.H.; Kim, M.-K.; Song, Y.-S. In vitro cytotoxicity of SiO₂ or ZnO nanoparticles with different sizes and surface charges on U373MG human glioblastoma cells. *Int. J. Nanomed.* **2014**, *9*, 235–241.

66. CFR-Code of Federal Regulations Title 21. Available online: https://www.accessdata.fda.gov/scripts/cdrh/cfdocs/cfcfr/CFRSearch.cfm?fr=73.2575 (accessed on 18 May 2020).

67. Xiao, C.; Lachance, B.; Sunahara, G.; Luong, J.H.T. Assessment of cytotoxicity using electric cell-substrate impedance sensing: Concentration and time response function approach. *Anal. Chem.* **2002**, *74*, 5748–5753. [CrossRef]

68. Xiao, C.; Luong, J.H.T. On-line monitoring of cell growth and cytotoxicity using electric cell-substrate impedance sensing (ECIS). *Biotechnol. Prog.* **2003**, *19*, 1000–1005. [CrossRef]

69. Male, K.B.; Lachance, B.; Hrapovic, S.; Sunahara, G.; Luong, J.H.T. Assessment of cytotoxicity of quantum dots and gold nanoparticles using cell-based impedance spectroscopy. *Anal. Chem.* **2008**, *80*, 5487–5493. [CrossRef] [PubMed]

70. Buzid, A.; Shang, F.J.; Reen, F.J.; Muimhneachain, E.O.; Clarke, S.L.; Zhou, L.; Luong, J.H.T.; O'Gara, F.; McGlacken, G.P.; Glennon, J.D. Molecular signature of *Pseudomonas aeruginosa* with simultaneous nanomolar detection of quorum sensing signaling molecules at a boron-doped diamond electrode. *Sci. Rep.* **2016**, *6*, 30001. [CrossRef]

71. Buzid, A.; Muimhneachain, E.O.; Reen, F.J.; Hayes, P.E.; Pardo, L.M.; Shang, F.J.; O'Gara, F.; Sperry, J.; Luong, J.H.T.; Glennon, J.D. Synthesis and electrochemical detection of a thiazolyl-indole natural product isolated from the nosocomial pathogen *Pseudomonas aeruginosa*. *Anal. Bioanal. Chem.* **2016**, *40*, 6361–6367. [CrossRef]

72. Buzid, A.; Luong, J.H.T.; Reen, F.J.; O'Gara, F.; Glennon, J.D.; McGlacken, G.P. Rapid electrochemical detection of *Pseudomonas aeruginosa* signaling molecules by boron-doped diamond electrode. *Meth. Mol. Biol.* **2018**, *1673*, 107–116.

73. Hoque, J.; Akkapeddi, P.; Yarlagadda, V.; Uppu, D.S.; Kumar, P.; Haldar, J. Cleavable cationic antibacterial amphiphiles: Synthesis, mechanism of action, and cytotoxicity. *Langmuir* **2012**, *28*, 12225–12234. [CrossRef]

74. Zhou, C.; Wang, F.; Chen, H.; Li, M.; Qiao, F.; Liu, Z.; Hou, Y.; Wu, C.; Fan, Y.; Liu, L.; et al. Fluorescence resonance energy transfer-based wash-free bacterial imaging and antibacterial application using a cationic conjugated polyelectrolyte. *ACS Appl. Mater. Interf.* **2016**, *8*, 4242–4249. [CrossRef] [PubMed]

75. Ling, C.A.; Mahmud, S.; Bakhori, S.K.M.; Sirelkhatim, A.; Mohamad, D.; Hasan, H.; Seeni, A.; Rahman, R.A. Effect of surface modification and UVA photoactivation on antibacterial bioactivity of zinc oxide powder. *Appl. Surf. Sci.* **2014**, *292*, 405–412.

76. Kirkinezos, I.G.; Moraes, C.T. Reactive oxygen species and mitochondrial diseases. *Semin. Cell Dev. Biol.* **2001**, *12*, 449–457. [CrossRef]

77. Lépine, F.; Déziel, E.; Milot, S.; Rahme, L.G. A stable isotope dilution assay for the quantification of the Pseudomonas quinolone signal in *Pseudomonas aeruginosa* cultures. *Biochim. Biophys. Acta* **2003**, *1622*, 36–41. [CrossRef]

78. Reen, F.J.; Mooij, M.J.; Holcombe, L.J.; McSweeney, C.M.; McGlacken, G.P.; Morrissey, J.P.; O'Gara, F. The Pseudomonas quinolone signal (PQS), and its precursor HHQ, modulate interspecies and interkingdom behaviour. *FEMS Microbiol. Ecol.* **2011**, *77*, 413–428. [CrossRef] [PubMed]

79. Sordé, R.; Pahissa, A.; Rello, J. Management of refractory *Pseudomonas aeruginosa* infection in cystic fibrosis. *Infect. Drug Resist.* **2011**, *4*, 31–41. [CrossRef] [PubMed]

80. Govan, J.R.; Deretic, V. Microbial pathogenesis in cystic fibrosis: Mucoid *Pseudomonas aeruginosa* and *Burkholderia cepacian. Microbiol. Rev.* **1996**, *60*, 539–574. [CrossRef]

81. Haussler, S.; Becker, T. The pseudomonas quinolone signal (PQS) balances life and death in *Pseudomonas aeruginosa* populations. *PLoS Pathog.* **2008**, *4*, e1000166. [CrossRef]

82. Livermore, D.M. The need for new antibiotics. *Clin. Microbiol. Infect.* **2004**, *10* (Suppl. 4), 1–9. [CrossRef]

83. Dong, H.; Li, C.M.; Chen, W.; Zhou, Q.; Zeng, Z.X.; Luong, J.H.T. Sensitive amperometric immunosensing using polypyrrolepropylic acid films for biomolecule immobilization. *Anal. Chem.* **2006**, *78*, 7424–7431. [CrossRef]

84. Shang, F.J.; Zhou, L.; Mahmoud, K.A.; Hrapovic, S.; Liu, Y.; Moynihan, H.A.; Glennon, J.D.; Luong, J.H.T. Selective nanomolar detection of dopamine using a boron-doped diamond electrode modified with an electropolymerized sulfobutylether-beta-cyclodextrin-doped poly(N-acetyltyramine) and polypyrrole composite film. *Anal. Chem.* **2009**, *81*, 4089–4098. [CrossRef] [PubMed]